Record of methane emissions from the West Svalbard continental margin during the last 23.500 yrs revealed by delta C-13 of benthic foraminifera

Panieri Giuliana [1, 2, *] , James Rachael H. [3], Camerlenghi Angelo [4], Westbrook Graham [3, 5, 6],
Consolaro Chiara [1, 7], Cacho Isabel [8], Cesari Valentina [2], Sanchez Cervera Cristina [8]

[1] UiT Arctic Univ Norway, CAGE Ctr Arctic Gas Hydrate Environm & Climate, N-9037 Tromso, Norway.
[2] CNR ISMAR, I-40129 Bologna, Italy.
[3] Univ Southampton, Natl Oceanog Ctr, Southampton SO14 3ZH, Hants, England.
[4] OGS Ist Nazl Oceanog & Geofis Sperimentale, I-34010 Trieste, Italy.
[5] Univ Birmingham, Sch Geog Earth & Environm Sci, Birmingham B15 2TT, W Midlands, England.
[6] IFREMER, Ctr Brest, F-29280 Plouzane, France.
[7] Univ Plymouth, Sch Geog Earth & Environm Sci, Plymouth PL4 8AA, Devon, England.
[8] Univ Barcelona, Fac Geol, Dept Estratig Paleontol & Geociencies Marines, GRC Geociencies Marines,
E-08028 Barcelona, Spain.

* Corresponding author : Giuliana Panieri, email address : giuliana.panieri@uit.no

Abstract :

The values of delta C-13 in benthic foraminifera have been measured in a gas-hydrate-bearing sediment core collected from an area of active methane venting on the Vestnesa Ridge (West Svalbard continental margin) to reconstruct the local history of methane emissions over the past 23.500 yrs BP. The chronostratigraphic framework of the core has been derived from AMS C-14 dates and biostratigraphic analysis. While foraminifera from some intervals have delta C-13 within the normal marine range (0 to-1%.), five intervals are characterized by a much lower delta C-13, as low as -17.4%.. These intervals are interpreted to record the incorporation of C-13-depleted carbon in the presence of methane emissions at the seafloor during biomineralization of the carbonate foraminiferal tests and subsequent secondary mineralization. Methane emission events (MEE) occur from the Last Glacial Maximum (LGM) to the Holocene, with the most prominent one, in terms of delta C-13 depletion, predating the Bolling-Allerod Interstadial (GI-1 in the Greenland ice core record). The lack of correlation between the values of delta C-13 and delta O-18, however, appears to preclude warming of bottom waters as the principal control on methane release. Rather, it seems likely that methane release is a consequence of episodicity in the supply of gas to the hydrate system and in the processes that enable methane gas to migrate through the hydrate stability field to the seabed, or of other geological processes still under debate.

Highlights

► Negative $\delta^{13}C$ in benthic foraminifera indicates methane emissions in the Arctic. ► Methane emissions have occurred at least over the past 23.5 ka in the Vestnesa Ridge. ► Methane emission events show an apparent correlation with climatic events. ► Geological processes may control the supply rate of methane to the seabed.

1. Introduction

Gas hydrate occurs naturally in marine sediments, where methane gas is available and temperatures are relatively low and pressure is relatively high. Estimates of the quantity of hydrate-bound gas in marine sediments range from 500 to 3000 Gt of carbon (Buffett and Archer, 2004); additionally, hydrates are frequently underlain by free gas reservoirs that may contain another ~1800 Gt of carbon (Buffet and Archer, 2004). Together, the hydrate and underlying free gas reservoirs comprise almost half of the Earth's organic carbon. Release of methane from hydrate may have contributed to rapid climate change in the past (e.g. Nisbet and Chappellaz, 2009), and it is considered to be a significant natural hazard because hydrate decomposition could destabilize sediments, creating landslide and tsunami risk (Berndt et al., 2009).

Most climate models predict a rapid increase in Arctic air and surface waters temperatures within the next decades (IPCC, 2007). The West Spitsbergen Current in the eastern Fram Strait showed a net increase in temperature of 0.8°C between 1997 and 2010 (Beszczynska-Möller et al., 2012) and, for the period 1975-2008, a net increase of 1°C of the water at 400 m depth was demonstrated in the region of occurrence of plumes of gas bubbles from the seabed (Westbrook et al., 2009). There have been a number of recent discoveries of methane emissions from the seafloor in the Arctic Ocean in water depths up to 400 m or so (Shakova et al., 2009, 2010; Westbrook et al., 2009; Berndt et al., 2013; Shaling et al., 2014), and some authors have suggested that these may, in part, be related to warming-induced dissociation of hydrate (Westbrook et al., 2009; Reagan and Moridis, 2009; Thatcher et al., 2013; Biastoch et al., 2011; Isaksen et al., 2011).

There are also, however, methane emissions from pockmarks in water depths greater than 800 m, in the area of the Vestnesa Ridge west of Svalbard (Hustoft et al., 2009; Bunz et al., 2012). Water at this depth and deeper is of Arctic origin, with a temperature of less than 0°C (Cokelet et al., 2008). This water does not show the same degree of temporal variability as the West Spitsbergen current (e.g. Cokelet et al., 2008; Beszczynska-Möller et al., 2012), but the data are sparse and the time series is short. Establishing whether there are any links between climate change and gas venting from these features within the gas hydrate stability zone (GHSZ) is, therefore, important for assessing the effects of future climate change in the Arctic.

One way to reconstruct past marine methane emissions is by carbon isotope (δ^{13}C) analysis of benthic foraminifera (e.g. Kennett et al., 2000). Recent work has shown that significant δ^{13}C depletion occurs in benthic foraminifera shells living adjacent to active methane seeps with low δ^{13}C (Rathburn et al., 2003; Hill et al., 2004; Panieri et al., 2009, 2012, 2014). Thus, in an effort to reconstruct the record of past methane emissions from the Arctic seafloor, we have conducted δ^{13}C analyses of benthic foraminifera, together with other geochemical, micropalaeontological and sedimentological analyses, on a hydrate-bearing sediment core collected from the Vestnesa Ridge in the West Svalbard continental margin. The data are used to establish a chronology of climate conditions and they reveal that methane emissions have occurred and varied significantly over the past ~23,500 years.

2. GEOLOGICAL SETTING

Vestnesa Ridge is located on <19.6 Ma oceanic crust of the eastern spreading segment of the Molloy Ridge in the eastern Fram Strait, offshore western Svalbard (Ritzmann et al.,

2004; Engen et al., 2008) (Fig. 1). The basaltic basement is overlain by sediments, up to 6

km thick (Crane et al., 2001), which consist of silty turbidites and muddy-silty

contourites of late Weichselian and Holocene age, deposited at an average rate of 9.6

cm.ka^{-1} since 19 ka before present (Howe et al., 2008). The upper part of the sediment

sequence includes glacigenic sediments, which reflect the intensification of Northern

Hemisphere glaciations since the late Pliocene (Moran et al., 2006). Pre-glacial and

glacial sediments are permeated by free gas and gas hydrate, the presence of which is

revealed by a prominent bottom simulating reflector (BSR) in seismic profiles, with

increased seismic velocity above the BSR, caused by the presence of hydrate, and a large

reduction in seismic velocity beneath it, caused by the presence of free gas (Posewang

and Mienert, 1999; Westbrook et al., 2008; Hustoft et al., 2009; Chabert et al., 2011). A

plume of gas bubbles from a pockmark on the Vestnesa Ridge was first observed in 2008

from RRS James Clark Ross cruise JR211 (reported in Hustoft et al., 2009, together with

later observations). The pockmark, with a diameter of 600 m, is one of many along the

ridge and lies at the top of a gas chimney (Hustoft et al., 2009; Petersen et al., 2010; Bünz

et al., 2012). The formation of chimneys such as these and the accompanying migration

of free gas is likely to have occurred over thousands of years (Liu and Flemings, 2007;

Hustoft et al., 2009). The gas venting at Vestnesa Ridge has a deep, thermogenic origin

(Smith et al., 2014), and the combination of cold temperatures in the water column makes

the top of the hydrate stability zone in the water column anomalously shallow (about 300

m), thus allowing for the possibility that hydrate-coated gas bubbles can contribute to the

transfer of methane into the atmosphere (Smith et al., 2014).

3. MATERIALS AND METHODS

3.1 Sample Collection

The sediment gravity core GC-26 (386 cm in length, Fig. 2) was collected very close to the site of the gas-bubble plume detected with a Simrad EK60 'fishfinder' sonar at the western edge of the pockmark on the crest of the Vestnesa Ridge (Fig. 1), in a water depth of 1210 m, during RRS *James Clark Ross* cruise JR211 in September 2008. The core was navigated to the bubble plume using ultra short baseline acoustic positioning while the ship maintained its station using dynamic positioning. Active venting of bubbles was observed at the time the core was collected, but repeated visits to the area indicated that venting was episodic.

The core was split, opened, and subsampled onboard immediately after retrieval. Samples for hydrocarbon gas analysis (*ca*. 3 cm^3) were processed using the headspace technique (Hoehler et al., 2000). Sediment pore-fluids were immediately extracted in a glove bag under a N_2-atmopshere by pressure filtration through 0.2 μm cellulose acetate filters. Samples of gas hydrate were extracted from the core and stored wrapped in cotton in liquid nitrogen.

3.2 Porefluid, hydrocarbon and porosity analysis

Total alkalinity (TA) concentrations were determined onboard immediately after porefluid extraction by manual titration (Ivanenkov and Lyakhin, 1978), while concentrations of all other chemical species were determined onshore at the National Oceanography Centre in Southampton, UK. Sulfate (SO_4^{2-}) concentrations were measured by ion chromatography (Dionex ICS2500). The reproducibility of these measurements was determined by repeat analysis of a seawater standard as well as single

anion solutions and is better than 1%. Headspace methane abundance was measured on a gas chromatograph (HP Agilent 6850) equipped with a 30 m long 0.32 mm wide column and flame ionisation detector. Note that depressurisation and warming of the core during retrieval are likely to have led to degassing, so the concentration of methane we report is considered to be the minimum. Sediment porosity was calculated from the loss of water after drying of the sediment at 110 °C assuming a dry solid density of 2.65 g. cm^{-3}.

3.3 Micropalaeontology

Sixty three sediment samples were collected with variable spacing from the top to the bottom of the core for micropaleontological and carbon and oxygen stable isotope analyses. Samples were washed through a 63 μm mesh size sieve, and oven dried at 40 °C. The dry residue, or an aliquot obtained with a micro-splitter, was examined under binocular microscope to pick out benthic foraminifera. Where possible, approximately 300 specimens were identified to species level and counted.

3.4 Stable isotopes

Specimens for stable isotope analyses (δ^{13}C and δ^{18}O) were picked from the >100 μm size fraction and examined using light microscopy to determine if there was evidence of dissolution, diagenesis or postdepositional alteration. A selection of specimens was examined via Scanning Electron Microscopy (SEM) to further describe their preservation. Approximately 10 μg of foraminiferal tests, which corresponds to roughly 10 to 30 individuals, were selected for each mass spectrometer analyses. Samples were split in two and cleaned following two different protocols in order to evaluate the effects of any diagenetic carbonate attached to the foraminifera tests. The first set was crushed

and cleaned with methanol, which is the standard protocol for stable isotopes measurements. The second set of samples were cleaned using a more exhaustive protocol designed for measurements of trace elements (Pena et al., 2005) which is adapted from Boyle and Rosenthal (1996). For this protocol, the foraminifera were first gently crushed between clean glass plates to break open individual chambers. The cleaning steps comprise: 1) removal of clays, Mn–Fe oxides and other mineral phases by reductive cleaning; 2) oxidative cleaning to eliminate organic matter; and 3) weak acid leaching to remove remaining impurities from the shell surfaces. This protocol has proven to be efficient in removing the diagenetic carbonates attached to the foraminifera shell (Pena et al., 2008; Panieri et al., 2012). The SEM images reported here provide evidence as to the efficacy of this procedure for removal of carbonate overgrowths.

The carbon and oxygen stable isotope compositions of *Cassidulina neoteretis* (Table 1) and *Melonis barleeanum* were measured on a ThermoFinnigan MAT252 mass spectrometer coupled to a CarboKiel-II carbonate preparation device at the Serveis Cientifico-Técnics of the University of Barcelona. Analytical precision was estimated to be better than 0.03‰ for $\delta^{13}C$ and 0.08‰ for $\delta^{18}O$ by measuring the certified standard NBS-19. Isotope results are reported in standard delta notation relative to Vienna Peedee Belemnite (VPDB).

3.5 Radiocarbon Dates

AMS radiocarbon dates (Table 2) were obtained for samples at 29, 38,108, 153, 181, 321, 361, and 386 cm bsf. As planktonic foraminifera are scarce in this core, dates were measured on hand picked from > 100μm size fraction clean benthic (*Cassidulina neoteretis, Cassidulina laevigata, Melonis barleeanum*) and planktonic

(*Neogloboquadrina pachyderma, Turborotalia quinqueloba*) foraminiferal tests, which showed no evidence of calcitic overgrowths. The picked material was submitted for analysis at the National Ocean Sciences Accelerator Mass Spectrometry Facility (NOSAMS) radiocarbon laboratory at the Woods Hole Oceanographic Institution (USA). Radiocarbon ages were calibrated using the marine calibration curve Marin 09 (Reimer et al., 2013) and the program Calib 7.0 (Stuvier et al., 2014). The reservoir-age correction (☐R) used to convert ages in Calendar years BP was 400 years (Mangerud and Gulliksen, 1975). A regional correction of $\Delta R =105\pm24$ years was applied for mixed benthic and planktic and $\Delta R =7\pm11$ for planktic, following the recommendations by Bondevik and Gulliksen in Mangerud et al. (2006). The Marine Reservoir Correction Database in CALIB (http://calib.qub.ac.uk/marine/) gives a much lower reservoir age for the investigated area, but this was not used as the samples in this database are from shallow water sites or coastal (fjord) areas. Thus, a shift to younger ages is possible because of the uncertainties in reservoir age. In addition, ΔR may be higher for benthic foraminifera, compared to planktonic foraminifera, at this site, because the seafloor and upper ocean are located in different water masses.

4. RESULTS

4.1 Composition of sediments and porefluids

The sediments consist of grey/brown to dark grey clay, with occasional thin sandy layers in the uppermost 10 cm (Fig. 2). Gas hydrate was present below 193 cm below seafloor (cm bsf), in the form of thin, opaque ice-like plates interbedded with the sediments. Once the hydrate had dissociated, the sediments became soupy, but did not show signs of reworking. Gas hydrate dissociation in sediment cores upon recovery does not necessarily

imply intense reworking and stratigraphic disruption (e.g. Piñero et al., 2006; Kastner et al., 1995). Gas hydrates accumulate preferentially in coarser grained intervals that generate characteristic water-rich soupy layers (or mousse-like layers) which retain textural characteristcs and pore fluid composition upon dissociation in the core liner. The biostratigraphic record, and the results from 14C dating, with exceptions discussed below in this study, demonstrate that core GC-26 has retained a meaningful stratigraphic record, although the gas hydrate-bearing interval of the core most likely underwent significative expansion.

Concentrations of methane within the sediments are as high as ~2 mmol L^{-1} of porefluid, but they are close to zero above ~62 cm bsf (Fig. 2). The concentration of porefluid sulfate was close to that of seawater at the seawater-sediment interface (24.9 mmol L^{-1}), but fell to zero at ~62 cm bsf. Thus, the depth of SO_4^{2-} penetration coincides with increased levels of CH_4 (and TA), which suggests that anaerobic oxidation of CH_4 is the main driver of SO_4^{2-} consumption at the Vestnesa Ridge: $CH_4 + SO_4^{2-} \rightarrow HCO_3^- + HS^- + H_2O$ (Reeburgh, 1976; Boetius et al., 2000). Concentrations of Cl^- are close to that of bottom seawater (555 mM) in the uppermost sediments, but they are lower (as low as 381 mM) in the lowermost hydrate-bearing sediments, because of dissociation of hydrate. It should be noted that the SO_4^{2-} concentration measured in pore fluids from sediments recovered from close to the seafloor in a nearby box core (JR211 24) is higher (28.7 mmol L^{-1}) than measured at the top of this core (25 mmol L^{-1}), which suggests that part of the uppermost sedimentary record in core GC-26 is missing.

4.2 Micropalaeontolgy

Several intervals of the sediment core are almost barren of planktonic foraminifera,

whereas benthic foraminifera occur throughout the whole core. Of the benthic foraminifera assemblage data only those species, which have been identified before to provide crucial paleoceanographic information (Bauch et al., 2001; Wollenburg et al., 2004; Rasmussen et al., 2007; Ślubowska-Woldengen et al., 2007; 2008), are described and shown in Fig. 3.

Based on the most pronounced changes in the distribution pattern of the benthic foraminifera in response to climatic changes our record could be subdivided into four major intervals. From 384 to 282 cm bsf *Elphidium excavatum* together with *Cassidulina reniforme* and *Cassidulina neoteretis* are typical for arctic glaciomarine environments close to glaciers and ice caps (e.g., Hald et al., 1994; Hald and Korsun, 1997; Ślubowska-Woldenberg et al., 2007). The decreasing in the relative abundance of *Elphidium excavatum* towards the end of this interval is indicative of low salinity and cold bottom waters conditions characterizing the deglaciation at the end of the LGM, as suggested by Rasmussen et al. (2007).

Between ca. 282 and 145 cm bsf the foraminiferal assemblage dominated by *Cassidulina reniforme,* together with *Cassidulina neoteretis*, and *Melonis barleeanum* (in our record only present in the upper part of the interval) indicate increased advection of Atlantic Water and improved food supply. *Cassidulina reniforme* indicates salinities higher than those preferred by *Elphidium excavatum* (e.g., Hald and Korsun, 1997) and *Cassidulina neoteretis* indicates inflow of relatively warm Atlantic Water below cold and fresh polar surface waters (e.g., Mackensen and Hald, 1988; Rasmussen et al., 1996; Rytter et al., 2002; Jennings et al., 2004). This core interval therefore displays environmental conditions typical of the Bølling-Allerød (B-A) interstadial (14,650–12,850 cal yr BP) (Ślubowska-Woldenberg et al., 2007).

From about 145 to 112 cm bsf the gradual change in the foraminiferal assemblage is compatible with the Younger Dryas (YD) stadial (12,850–11,650 cal yr BP) with freshening of the bottom waters with abundant *Cassidulina reniforme*, whereas the low abundance of *Cassidulina neoteretis* indicates that the influence of Atlantic water at depth was reduced (Rasmussen et al., 2007).

The interval between 112 cm bsf to the top of the core is characterized by a pronounced change in the benthic foraminiferal assemblage that is indicative of the marked warming at the beginning of the Holocene (11,650 cal yr BP–present; Holocene) (Mangerud et al., 1974; Björck et al., 1998). The warming is characterized by an increase in the relative abundance of *Cibicidoides wuellerstorfi* and Agglutinants, together with *Cassidulina reniforme* and *Cassidulina neoteretis* and *Melonis barleeanum* and less abundant *Nonionella labradorica*. *Cibicidoides wuellerstorfi* is typically dominant the climatic change from glacial to interglacial water-mass conditions in the Nordic seas and is a well define biostratigraphic event in this area (Belanger, 1982; Struck, 1995; Rasmussen et al., 2007) and which becomes more abundant only after 12 cal Kyr in the Nordic seas (Bauch et al., 2001). The agglutinants are moderately abundant in the Holocene fauna as suggested by Wollenburg et al. (2004). The high percentage of *Cassidulina neoteretis* and *Cassidulina reniforme* are indicative of enhanced inflow of subsurface Atlantic Water into the area and the presence of *Nonionella labradorica* indicate that the environment is strongly influenced by the Arctic Coastal Front, but with higher salinity and bottom water temperature than during the Younger Dryas (Ślubowska-Woldenberg et al., 2007).

The foraminiferal tests examined by scanning electron microscopy (SEM) are generally well-preserved. Most specimens showed no obvious diagenetic overgrowths,

but a small amount of calcitic overgrowth or coating was evident on some tests mainly in the interval between 250 and 300 cm (Fig. 4).

4.3 Chronology

An age model for the core has been constructed from: 1) AMS ^{14}C dating; 2) by comparison of the most pronounced changes in the distribution pattern of the benthic foraminifera species in core GC-26 with other sediment cores from the West Svalbard continental margin (Bauch et al., 2001; Wollenburg et al., 2004; Rasmussen et al., 2007; Ślubowska-Woldengen et al., 2007; 2008); 3) correlation of the resulting chronostratigraphy with the NGRIP δ^{18}O record (Björck et al., 1998). In spite of dissociation of hydrate in the lowermost part of the core after its recovery, core GC-26 provides a continuous sedimentary succession from ~23,500 years ago (estimated age for the bottom of the core) to the Holocene.

4.3.1 AMS ^{14}C dating

The eight ages obtained show an increasing trend down core consistent with the chronostratigraphic tie points described above with the exception of samples at 38 cm bsf (14,200 ±390 yr BP) and at 108 cm bsf (17,160 ± 478 a BP) that are older than the age of the deeper samples. The reason for the older age at 108 cm bsf is the negative value of the δ^{13}C (-10.98 ‰, Table 1) of the dated specimens. This suggests that the foraminiferal carbonate analysed for the AMS ^{14}C dating contains old carbon isotopes up-taken from the marine reservoir locally enriched by methane seeping from a geological reservoir (Gulin et al., 2003). There is no δ^{13}C information for the sample at 38 cm bsf. Because

this sample was taken only a few cm above the uppermost ^{13}C-depleted sample at 45 cm

bsf, a similar explanation for the old age can be provided as for sample at 108 cm bsf.

Therefore, these ages are not used in the age model for the core GC-26. The resulting age

model defines clearly a part of the core, matching with the gas hydrate bearing part, in

which an extremely rapid apparent sedimentation rate can be explained with sediment

expansion due to gas hydrate phase change in the core liner during recovery.

4.3.2 Chronostratigraphic tie points

As described in section 'Micropaleontology', on the basis of the relative abundance of

different foraminiferal species, a number of chronostratigraphic tie points to other

sediment cores from the West Svalbard continental margin, for which absolute

chronologies based on AMS ^{14}C dates are available, can be identified (Fig. 5). In

summary, the interval between 292 and 145 cm bsf includes the age range from 14,650 to

12,850 cal yr BP (Bølling and Allerød interstadials), from 145 to 112 cm we can locate

the Younger Dryas stadial (12,850–11,650 cal yr BP), while the Holocene (11,650 cal yr

BP to present) is located from 112 cm bsf to the top of the core (Fig. 5) .

4.3.3 Linkage to the NGRIP $\delta^{18}O$ record

An additional control on the chronostratigraphy of core GC-26 can be obtained by

comparing its tie points and AMS ^{14}C dates with the age-controlled δ^{18}O record of the

Greenland ice core GISP2. This provides a number of additional tie points assuming a

continuous and constant sedimentation rate at least until the beginning of the Holocene.

(Fig. 5).

4.4 Stable isotope composition of benthic foraminifera

Many of the δ^{13}C values measured in the calcitic skeleton of the benthic foraminifera are significantly lower (as low as -17.4‰) than those expected for foraminifera recovered from the same region in sites unaffected by methane seepage (0-1‰; Wollenburg et al., 2001) (Fig. 5). The low δ^{13}C values are obtained both for tests cleaned using standard stable isotope protocol and for tests cleaned using the more intensive procedure. Tests cleaned using the latter procedure have higher δ^{13}C values, by up to 8‰, but these are still lower than values for 'normal' marine carbonates. These data indicate that while benthic foraminifera living in methane seep environments are affected by cryptocrystalline overgrowths (only revealed under SEM), these overgrowths could not have formed after the sediments were deposited, as the low δ^{13}C values occur in discrete stratigraphic intervals and are separated by values in the normal marine range. Moreover, these intervals do not coincide with present-day methane seepage, which occurs throughout sediments below ~62 cm bsf. As the pattern of variability in δ^{13}C is the same for both sample sets, this strongly suggests that primary and secondary mineralization must have occurred at about the same time.

The older age of samples from 108 cm bsf with δ^{13}C = -10.98‰ is a further evidence that the benthic foraminifera calcified using carbon from a reservoir that was significantly different from seawater.

Comparing the δ^{13}C values of *Melonis barleeanum* and *Cassidulina neoteretis* it can be noted that the trends are similar, but the former species shows less pronounced anomalies in δ^{13}C. Although we cannot entirely exclude the possibility that this is due to the small number of *Melonis barleeanum* tests, it is more likely that this difference reflects differences in metabolic activity, i.e. vital effects (Urey et al., 1951; McCorkle et

al., 1990, 1997), as previously reported by Panieri et al. (2012) for other species. Both of these species of benthic foraminifera therefore appear to have the capability to independently record methane emissions.

The $\delta^{18}O$ values measured in the benthic foraminifera do not exhibit significant variations throughout the core. Values obtained for *Cassidulina neoteretis* using both cleaning protocols are usually between ~4.5 and ~5.5‰, whereas values for *Melonis barleenaum* are slightly lower (3.8 to 4.7 ‰).

5. DISCUSSION

Stable isotope in benthic foraminifera

In the recent years, negative carbon-isotopic compositions of benthic foraminiferal tests from methane seep environments, has bee used to indicate that some of these species record distinct ^{13}C-depletions inherited from methane (Barbieri and Panieri, 2004, de Garidel-Thoron et al., 2004, Hill et al., 2003, Hill et al., 2004, Keigwin, 2002, Kennett et al., 2000, Martin et al., 2007, Martin et al., 2010, Panieri, 2005, Panieri et al., 2009, Panieri et al., 2012, Panieri et al., 2014; Rathburn et al., 2000, Sen Gupta and Aharon, 1994, Sen Gupta et al., 1997 and Wefer et al., 1994). The variations in $\delta^{13}C$ of foraminiferal tests at the seep sites are likely the result of calcification in the presence of a ^{13}C-depleted DIC and probably ingestion of ^{13}C-depleted methanotrophic microbes on which foraminifera feed. Thus, benthic foraminifers in methane seep environments likely preserve geochemical information from which past methane emission events may be reconstructed.

The $\delta^{13}C$ values measured in the calcitic skeleton of the benthic foraminifera in core GC-26 are significantly lower (as low as -17.4‰) than those expected for foraminifera

recovered from the same region in sites unaffected by methane seepage (0/-1‰; Wollenburg et al., 2001) (Fig. 5). We believe that those negative values reflect a local $\delta^{13}C$ due to process, as methane release, that influence the investigated area and are not related to global average $\delta^{13}C$ DIC changes due to perturbation in the global carbon cycle or water masses.

5.1 Methane Emission Events (MEEs)

Five 'methane emission events' (MEEs) can be recognized in core GC-26 (Fig. 5); these are identified by one or more samples with $\delta^{13}C$ markedly outside the normal marine range, and separated by at least one sample within the range. As discussed in Section 4.4, these anomalies appear to be in a large part produced by biomineralization of carbonate foraminiferal tests in the presence of methane emissions at the seafloor of the Vestnesa Ridge.

MEE5, at the bottom of the core within the LGM, is represented by only one sample. MEE 4 is the strongest and most long-lasting anomaly (less than 700 years in duration), pre-dating the Bølling-Allerød Interstadial or GI-1 event in the Greenland ice-core isotope stratigraphy (Björck et al., 1998) with onset close to 15,600 300 yr BP. This event pre-dated also the Meltwater Pulse 1A (mwp-1A) (Fairbanks, 1989; Hanebuth et al., 2000), for which evidence has been found in sediment cores further to the south of our study area along the West Svalbard margin (Lucchi et al., 2013). MEE 3 occurs a few hundred years after the Younger Dryas Stadial (GS-1) (Walker et al., 1999; Lowe, 2001). MEE 2 coincides with the early Holocene warming of surface water in the Nordic seas and in the bottom waters on the Arctic Ocean shelf (Lubinski et al., 2001; Ślubowska-Woldengen et al., 2007). It is possible that MEE2 and MEE3 are part of the same event,

as they are separated by only one sample with normal $\delta^{13}C$. The youngest MME 1 is probably incompletely recovered, because of the missing core top.

The five MEEs indicate that methane emissions have been occurring, even if with some interruptions, over a period of about 23,500 years in the Vestnesa Ridge. The benthic foraminifera record the methane seep when they live exposed to it. The reason why *Cassidulina neoteretis* recorded more/less depleted $\delta^{13}C$ during the MEEs throughout the core is unclear. It is possible that □he different amplitudes of the MEEs are related to differences in the venting characteristics. More depleted $\delta^{13}C$ due to active methane venting with activity particularly high and prolonged in time. Interestingly, MEE 4, which is the strongest, is also the most long-lasting anomaly (ca. 700 years in duration). On the contrary, less depleted $\delta^{13}C$ might be due to diffusive, even if constant, methane emissions. Similar $\delta^{13}C$ values for MEE 3, 2 and 1 raised a question: whether similar values are indicative of similar methane source or similar amount of gas. Any of the studies conducted so far provided clear relationship between the source and/or amount of methane and the documented negative $\delta^{13}C$ anomalies in benthic foraminifera. If this will be defined within other studies, the depletion and variability in foraminiferal $\delta^{13}C$ values it is possible that will be related to the strength of venting activity.

5.2 Linkage between MEEs and climate change?

At first sight, there is an apparent association between the five methane emission events and global or regional climatic events. If, however, bottom-water temperature changes were the primary cause of methane emissions, then we would expect to see a good correlation between the benthic foraminiferal $\delta^{18}O$ and $\delta^{13}C$ values, with periods of warming (higher $\delta^{18}O$) associated with methane release (lower $\delta^{13}C$). Although there is

an apparent correlation between $\delta^{18}O$ and $\delta^{13}C$ in *Melonis barleeanum* ($r^2 = 0.74$), there

is no relationship between these two parameters in *Cassidulina neoteretis*, cleaned using

either protocol (Fig. 5). Moreover, it is important to note that there are no significant

changes in the $\delta^{18}O$ record in Core GC-26. Other records for deep and intermediate water

depths in the Nordic seas (Meland et al., 2008) and also on the West Svalbard margin

(Rasmussen et al., 2007), in the Western Barents Sea (Groot et al., 2014), also indicate

that no abrupt changes in temperature occurred in bottom waters between the LGM to the

Holocene. During the Holocene, the strength of Atlantic water inflow into the northern

North Atlantic has varied, although with smaller amplitude than recorded for the glacial–

interglacial scale changes (e.g., Klitgaard-Kristensen et al., 2001; Risebrobakken et al.,

2003; Hald et al., 2007). Other marine records in the Barents Sea region have reported

that these smaller variations in the intensity of Atlantic water inflow during the Holocene

still have a strong impact on climate at the high northern latitudes (e.g., Duplessy et al.,

2001; Lubinski et al., 2001; Sarnthein et al., 2003; Slubowska-Woldengen et al.,2007).

In the Arctic Ocean there are several evidence that indicate a massive release of methane

during the deglaciation. A cluster of craterlike depressions in the central Barents Sea has

been interpreted as formed by eruption of free gas from gas hydrate dissociation when

grounded ice retreated from the area, i.e., after approximately 15 ka (Elverhoi et al.1990).

Following a rapid deglaciation, decomposition of gas hydrates added large volumes of

free gas, which eventually broke through the thinning seal of hydrates (Solheim and

Elverhøi, 1993). U-Th dating on methane-derived carbonate crusts on the Norwegian

continental shelf, including sites in the North Sea, the Norwegian Sea and the Barents

Sea, indicate that methane seepage along the northern Norwegian margin was most active

between 14 to 7ka after the collapse of the Scandinavian ice sheet and deglaciation of the

area that took place at about 15 ka. The methane flux for the carbonate crust formation

was likely provided by the dissociation of methane hydrates that extensively formed in

underlying sediments during the last glacial period, but became unstable due to

depressuring effects of retreating ice sheet (Crémière et al., 2014).

Although there is no obvious direct link between the episodic venting of methane at the

Vestnesa Ridge and climate change, the possibility of a delayed release of methane from

hydrate in response to warming should be considered. At the water depth of 1200 m, the

seabed is always well inside the GHSZ in the range of water temperature for the northern

Atlantic (Thatcher et al., 2013). The lower boundary of the GHSZ lies about 200 m

beneath the seabed where the temperature is high enough for hydrate not to be stable.

Evidently, pathways for migration of gas through the chimney exist, as demonstrated by

the present-day emission of free gas from the pockmark. These pathways could be

created by the invasion of gas at high pressure, combined with the increase in the salinity

of pore water as hydrate is formed, which restricts the formation of more hydrate at a

given depth until, with time, diffusion decreases the salinity (Liu and Flemings, 2007).

An increase in temperature could sustain a pathway for a longer period or rejuvenate gas

migration by the dissociation of hydrate already formed. There would, however, be a time

lag of up to several hundred years, for a significant effect from a change in temperature at

the seabed to diffuse downward (cf. Taylor et al., 2005) and so the shallower parts of the

pathway system would be more quickly and strongly affected than the deeper parts. So, it

might be the case that warming of the seabed could affect the uppermost parts of these

migration pathways, but the lack of clear evidence of warming, such as a temporal

correlation between the δ^{13}C and δ^{18}O records, even with a time lag, make this unlikely.

5.3 Other potential causes of MEEs

The episodicity of the methane emissions may have one or more geological causes, creating variations in the rate of migration of gas into the region beneath the chimney (Hustoft et al., 2009) and variability in the processes that enable methane to migrate through the GHSZ in features such as the gas chimney that lies beneath the pockmark. Some may produce apparent rather than real episodicity. The seep sites are commonly around the margins of large pockmarks, as is the seep site reported here. An explanation for this is that the migration pathways to an individual seep become blocked, over time, by the formation of authigenic carbonate, which stimulates the migration of gas pathways in sediment not already invaded by authigenic carbonate, leading to a general outward migration away from the earliest seep sites. When a switch occurs, the area most strongly affected by methane seeping into the water will change and so the record of methane in the benthic foraminifera will change as their proximity to the active seep changes. This hypothesis could be verified by coring different locations over the pockmark, which is about 500 m in diameter.

6. SUMMARY

A continuous sedimentary record spanning from 23,5 ka BP to the Holocene has been recovered in a gas hydrate-bearing sediment core from a pockmark underlain by a gas chimney on Vestnesa Ridge (Fram Strain, West Svalbard margin). The seafloor at the coring site is currently subject to methane venting. In spite of the sediment disturbance induced by the dissociation of gas hydrate in the core and the scarce amounts of calcareous foraminifera, the chronology of the core has been reconstructed by comparison of its biostratigraphic record with other dated cores from the surrounding

area, by eight AMS ^{14}C dates, and correlation with the GISP2 δ^{18}O ice core record.

The δ^{13}C record extracted from benthic foraminifera reveals negative anomalies as low as − 17.4 ‰. These negative anomalies persist after the application of a cleaning protocol designed to remove any authigenic carbonate coatings from the foraminferal tests.

Five anomalies are identified, in which the δ^{13}C values of benthic foraminifera are significantly lower than those expected for foraminifera recovered from the same region in sites unaffected by methane seepage. Anomalies are separated by at least one sample with normal marine δ^{13}C (0 - 1‰) and are, therefore, interpreted to represent five methane emission events (MEEs), occurring at the site during the last 23,500 years BP.

The MEEs show an apparent correlation with global or regional climatic events, but the δ^{18}O record from the benthic foraminifera provides no evidence of correlated increases of bottom-water temperature that might have induced gas hydrate dissociation. Therefore we interpret the MEEs as the result of one or more geological processes controlling the supply of methane to the seabed creating a real or apparent variation in methane emissions over time.

REFERENCES

Barbieri, R., Panieri, G., 2004. How are benthic foraminiferal fauna influenced by cold

seep? Evidence from the Miocene of Italy. Palaeogeography, Palaeoclimatology,

Palaeoecology 204, 255-275.

Bauch, H.A., Erlenkeuser, H., Spielhagen, R.F., Struck, U., Matthiessen, J., Thiede, J.,

Heinemeier, J., 2001. A multiproxy reconstruction of the evolution of deep and

surface waters in the subarctic Nordic Seas over the last 30,000 yr. Quaternary

Science Reviews 20, 659–678.

Berndt, C., Brune, S., Nisbet, E., Zschau, J., Sobolev S.V., 2009. Tsunami modeling of a

submarine landslide in the Fram Strait. Geochemistry, Geophysics, Geosystems 10,

Q04009, doi:10.1029/2008GC002292.

Beszczynska-Möller, A., Fahrbach, E., Schauer, U., Hansen, E., 2012. Variability in

Atlantic water temperature and transport at the entrance to the Arctic Ocean, 1997–

2010. ICES Journal of Marine Science 69, 852-863.

Biastoch, A., and 10 others, 2011, Rising Arctic Ocean temperatures cause gas hydrate

destabilization and ocean acidification. Geophysical Research Letters 38, L08602,

doi:10.1029/2011GL047222.

Björck, S., Walker, M.J.C., Cwynar, L.C., Johnsen, S., Knudsen, K., Lowe, J.J.,

Wohlfarth, B., INTIMATE Members, 1998. An event stratigraphy for the Last

Termination in the North Atlantic region based on the Greenland ice-core record: a proposal by the INTIMATE group. Journal of Quaternary Science 13, 283–292.

Boetius, A., Ravenschlag, K., Schubert, C. J., Rickert D., Widdel, F., Gieseke, A., Amann, R., Jorgensen, B. B., Witte, U., Pfannkuche, O., 2000. A marine microbial consortium apparently mediating anaerobic oxidation of methane. Nature, 407, 623-626.

Boyle, E.A., Rosenthal, Y., 1996. Chemical hydrography of the south Atlantic during the Last Glacial Maximum: Cd vs. δ^{13}C, in: Wefer, G., et al. (Eds.), The South Atlantic: Present and Past Circulation. Springer, New York, pp. 423–443.

Bünz, S., Polyanov, S., Vadakkepuliyambatta, S., Consolaro, C., Mienert, J., 2012. Active gas venting through hydrate-bearing sediments on the Vestnesa Ridge, offshore W-Svalbard. Marine Geology 332-334, 189-197. doi:10.1016/j.margeo.2012.09.012.

Buffett, B., Archer, D., 2004. Global inventory of methane clathrate: sensitivity to changes in the deep ocean. Earth and Planetary Science Letters 227, 185–199.

Chabert, A., Minshull, T.A., Westbrook, G.K., Berndt, C., Thatcher, K.E., Sarkar, S., 2011. Characterization of a stratigraphically constrined gas hydrate system along the western continental margin of Svalbard from ocean bottom seismometer data. Journal of Geophysical Research 116, B12102, doi: 10.1029/2011JB008211.

Cokelet, E.D., Tervalon, N., Bellingham J.G., 2008. Hydrography of the West Spitsbergen Current, Svalbard branch: Autumn 2001. Journal of Geophysical Research 113, C01006.

Crane, K., Doss, H., Vogt, P.R., Sundvor, E., Cherkashov, G., Poroshina, I., Joseph, D., 2001. The role of the Spitsbergen shear zone in determining morphology,

segmentation and evolution of the Knipovich Ridge. Marine Geophysical Research, 22, 153–205.

Crémière A., Lepland A., Sahy, D., Noble, S.R., Condon, D.J., Chand, S., Stoddart, D., Pedersen J.H., Sauer, S., Brunstad, H., Pedersen, R.B., Terje Thornes, T., 2014. Methane-derived carbonates as archives of past seepage activity along the Norwegian margin. Geophysical Research Abstracts, Vol. 16, EGU2014-13517, 2014 EGU General Assembly 2014.

Engen, Ø., Faleide, J.I., and Dyreng, T.K., 2008. Opening of the Fram Strait gateway: a review of plate tectonic constraints. Tectonophysics 450(1-4), 51-69.

Fairbanks, R.G., 1989. A 17000-years glacio-eustatic sea level record: influence of glacial melting rates on the Younger Dryas event and deep-ocean circulation. Nature 342, 637–742.

Gulin, S.B., Polikarpov, G.G., Egorov, V.N., 2003. The age of microbial carbonate structures grown at methane seeps in the Black Sea with an implication of dating of the seeping methane. Marine Chemistry 84, 67–72.

Hanebuth, T., Stattegger, K., Grootes, P.M., 2000. Rapid flooding of the Sunda shelf: a late-glacial sea-level record. Science 288, 1033-1035.

Hill, T.M., Kennett, J.P., Valentine, D.L., 2004. Isotopic evidence for the incorporation of methane-derived carbon into foraminifera from modern methane seeps, Hydrate Ridge, Northeast Pacific. Geochimica et Cosmochimica Acta 68, 4619–4627.

Hoehler F. K., Borowski C., Alperin M., Rodriguez N. M., Paull C. K., 2000. Model, stable isotope, and radiotracer characterization of anaerobic methane oxidation in gas hydrate-bearing sediments of the Blake Ridge, in: Proceedings of the Ocean

Drilling Program Scientific Results 164: College Station, TX (Ocean Drilling Program), pp. 79-85.

Howe, J.A., Shimmield, T.M., Harland, R., 2008. Late quaternary contourites and glaciomarine sedimentation in the Fram Strait. Sedimentology 55(1), 179-200.

Hughen, K., and 26 others, 2004. Marine04 marine radiocarbon age calibration, 0–26 cal kyr B.P. Radiocarbon 46, 1059–1086.

Hustoft, S., Bünz, S., Mienert, J., Chand, S., 2009. Gas hydrate reservoir and active methane-venting province in sediments on < 20 Ma young oceanic crust in the Fram Strait, offshore NW-Svalbard. Earth and Planetary Science Letters 284, 12-24.

IPCC, 2007, IPCC Fourth Assessment Report: Climate Change 2007. in: Solomon, S., Qin, D., Manning, M., Chen, M., Marquis, M., Averyt, K.B., Tignor, M., Miller, H.L. (Eds.), Contribution of Working Group I to the Fourth Assessment Report of the Intergovernmental Panel on Climate Change. Cambridge University Press, Cambridge, United Kingdom and New York, USA.

Isaksen, I.S.A., Gauss M., Myhre G., Anthony K.M.W., Ruppel, C., 2011. Strong atmospheric chemistry feedback to climate warming from Arctic methane emissions. Global Biogeochemical Cycles 25, GB2002, doi:10.1029/2010GB003845.

Ivanenkov V.N., Lyakhin Y.I., 1978. Determination of total alkalinity in seawater, in: Bordovsky, O.A., and Ivanenkov, V.N. (Eds.), Methods of hydrochemical investigations in the ocean, Nauka Publication House, Moscow, pp. 110-114.

Kastner M., Kvenvolden K.A., Whiticar M.J., Camerlenghi, A., and Lorenson T.D., 1995. Relationship between pore fluid chemistry and gas hydrates associated with

bottom-simulating reflectors at the Cascadia Margin, Sites 889 and 892. In Carson
B., Westbrook G.K., Musgrave R.J, and Suess E. (Eds.), Proceedings of the Ocean
Drilling Program, Scientific Results, 146:, College Station, TX (Ocean Drilling
Program) (Pt. 1):175-187.

Kennett, J.P., Cannariato, K.G., Hendy, I.L., Behl, R.J., 2000. Carbon isotopic evidence
for methane hydrate instability during quaternary interstadials. Science 288, 128-
133.

Liu, X., Flemings, P. B. 2007. Dynamic multiphase flow model of hydrate formation in
marine sediments. Journal of Geophysical Research 112, B03101,
doi:10.1029/2005JB004227.

Lowe, J.J., 2001. Abrupt climatic changes in Europe during the last glacial-interglacial
transition: The potential for testing hypotheses on the synchroneity of climatic
events using tephrochronology. Global and Planetary Change 30, 73-84.

Lubinski, D.J., Polyak, L., Forman S.L., 2001. Freshwater and Atlantic water inflows to
the deep northern Barents and Kara seas since ca. 13 ^{14}C ka: foraminifera and stable
isotopes. Quaternary Science Reviews 20, 1851–1879.

Lucchi, R.G., Camerlenghi, A., Rebesco, M., Colmenero-Hildago, E. Sierro, F.J.,
Sagnotti, L., Urgeles, R., Melis, R., Morigi, C., Barcena, L., Giorgetti, A., Villa, G.,
Persico, D., Flores, J.A., Rigual, A., Pedrosa, M.T., Macri, P., Caburlotto, A., in
press. Postglacial sedimentary processes on the Storfjorden and Kveithola trough
mouth fans: significance of extreme glacimarine sedimentation. Global and
Planetary Change, in press.

Mangerud, J., Andersen, S.T., Berglund, B.E., Donner, J.J., 1974. Quaternary
stratigraphy of Norden, a proposal for terminology and classification. Boreas 4,

109–128.

Mangerud, J., S. Bondevik, S. Gulliksen, A. K. Hufthammer, and T. Høisæter (2006),
Marine 14C reservoir ages for 19th century whales and molluscs from the North
Atlantic. Quaternary Science Reviews, 25, 3228−3245.

Mangerud, J., Gulliksen, S., 1975. Apparent radiocarbon ages of recent marine shells
from Norway, Spitsbergen and Arctic Canada. Quaternary Research 5, 263–273.

Martin, R.A., Nesbitt, E.A., Campbell, K.A., 2007. Carbon stable isotopic composition of
benthic foraminifera from Pliocene cold methane seeps, Cascadia accretionary
margin. Palaeogeography, Palaeoclimatology, Palaeoecology 246, 260–277.

McCorkle, D.C., Keigwin, L.D., Corliss, B.H., Emerson, S.R., 1990. The influence of
microhabitats on the carbon isotopic composition of deep-sea benthic foraminifera.
Paleoceanography 5, 161–185.

McCorkle, D.C., Corliss, B.H., Farn-ham, C.A., 1997. Vertical distributions and stable
isotopic compositions of live (stained) benthic foraminifera from the North
Carolina and California continental margins. Deep Sea Research Part I 44, 983–
1024.

Meland, Y.M., Dokken, T.M., Jansen, E., Hevrøy, K., 2008. Water mass properties and
exchange between the Nordic seas and the northern North Atlantic during the
period 23–6 ka: Benthic oxygen isotopic evidence. Paleoceanography 23, PA1210,
doi:10.1029/2007PA001416.

Moran, K., and 36 others, 2006. The Cenozoic palaeoenvironment of the Arctic Ocean.
Nature 441(1), 601-605, doi:10.1038/nature04800.

Nisbet, E.G., Chappellaz, J., 2009. Shifting gear, quickly. Science 324, 477-478.

Panieri G., Camerlenghi A., Cacho I., Sanchez Cervera C., Canals M., Lafuerza S.,

Herrera G., 2012. Tracing seafloor methane emissions with benthic foraminifera: Results from the Ana submarine landslide (Eivissa Channel, Western Mediterranean Sea). Marine Geology 291-294, 97–112.

Panieri, G., Camerlenghi, A., Conti, S., Pini, G.A., Cacho, I., 2009. Methane seepages recorded in benthic foraminifera from Miocene seep carbonates, Northern Apennines (Italy). Palaeogeography, Palaeoclimatology, Palaeoecology 284, 271–282.

Pena, L.D., Cacho, I., Calvo, E., Pelejero, C., Eggins, S., Sadekov, A., 2008. Characterization of contaminant phases in foraminifera carbonates by electron microprobe mapping. Geochemistry, Geophysics, Geosystems 9, Q07012. doi:10.1029/2008GC002018.

Pena, L.D., Calvo, E., Cacho, I., Eggins, S., Pelejero, C., 2005. Identification and removal of Mn–Mg-rich contaminant phases in foraminiferal tests: Implications for Mg/Ca past temperature reconstructions. Geochemistry, Geophysics, Geosystems 6, Q09P02, doi:10.1029/2005GC000930.

Petersen, C.J., Bünz, S., Hustoft, S., Mienert, J., Klaeschen, D., 2010. High-resolution P-Cable 3D seismic imaging of gas chimney structures in gas hydrated sediments of an Arctic sediment drift: Marine and Petroleum Geology 27, 1981-1994.

Piñero, E., Gràcia, E., Martínez-Ruiz, F., Larrasoaña, J.C., Vizcaino, A., and Ercilla, G., 2007. Gas hydrate disturbance fabrics of southern Hydrate Ridge sediments (ODP Leg 204): Relationship with texture and physical properties. Geo-Marine Letters 27, 279-288.

Posewang, J., Mienert, J., 1999. High-resolution seismic studies of gas hydrates west of Svalbard. Geo-Marine Letters 19, 150-156.

Rasmussen, T.L., Thomsen, E., Ślubowska, M.A., Jessen, S., Solheim, A., Koç, N., 2007. Paleoceanographic evolution of the SW Svalbard margin (76°N) since 20,000 ^{14}C yr BP. Quaternary Research 67, 100-114.

Rathburn, A.E., Pérez, M.E., Martin, J.B., Day, S.A., Mahn, C., Gieskes, J., Ziebis, W., Williams, D., Bahls, A., 2003. Relationships between the distribution and stable isotopic composition of living benthic foraminifera and cold methane seep biogeo-chemistry in Monterey Bay: California. Geochemistry, Geophysics, Geosystems 4, 1106, doi:10.1029/2003GC000595.

Reagan, M.T., Moridis, G.J., 2009. Large-scale simulation of methane hydrate dissociation along the West Spitsbergen Margin. Geophysical Research Letters 36, L23612, doi:10.1029/2009GL041332.

Reeburgh, W. S., 1976. Methane consumption in Cariaco Trench waters and sediments. Earth and Planetary Science Letters 28, 337-344.

Reimer, P. J., E. Bard, A. Bayliss, J. W. Beck, P. G. Blackwell, C. B. Ramsey, E. B. Caitlin, H. Cheng, R. L. Edwards, M. Friedrich, P. M. Grootes, T. P. Guilderson, H. Haflidason, I. Hajdas, C. Hatté, T. J. Heaton, D. L. Hoffmann, A. G. Hogg, K. A. Hugen, K. F. Kaiser, B. Kromer, S. W. Manning, M. Niu, R. W. Reimer, D. A. Richards, E. M. Scott, R. A. Staff, C. S. M. Turney, and J. van der Plicht (2013), Intcal13 and Marine13 radiocarbon age calibration curves 0 – 50,000 years cal bp. Radiocarbon, 55(4), 1869–1887.

Ritzmann, O., Jokat, W., Czuba, W., Guterch, A., Mjelde, R., Nishimura, Y., 2004. A deep seismic transect from Hovgård Ridge to northwestern Svalbard across the continental-ocean transition: a sheared margin study. Geophysical Journal International 157(2), 683-702.

Shakhova, N.E. Sergienko, V.I., Semiletov, I.P., 2009. The Contribution of the East Siberian Shelf to the Modern Methane Cycle. Herald of the Russian Academy of Sciences 79(3), 237–246

Shakhova, N.E., Semiletov, I., Salyuk, A., Yusupov, V., Kosmach, D. Gustafsson, O., 2010. Extensive methane venting to the atmosphere from sediments of the East Siberian Arctic Shelf. Science 327, 1246–1250.

Ślubowska, M.A., Koç, N., Rasmussen, T.L., Klitgaard-Kristensen, D., 2005. Changes in the flow of Atlantic water into the Arctic Ocean since the last deglaciation: Evidence from the northern Svalbard continental margin, 80°N. Paleoceanography 20(4) DOI: 10.1029/2005PA001141

Ślubowska-Woldengen, M., Rasmussen, T.L., Koç, N., Klitgaard Kristensen, D., Nilsen, F., Solheim, A., 2007. Advection of Atlantic Water to the western and northern Svalbard shelf since 17,500 cal yr BP. Quaternary Science Reviews 26, 463–478.

Ślubowska-Woldengen, M., Koç, N., Rasmussen, T.L., Klitgaard-Kristensen, D., Hald, M., Jennings, A.E., 2008. Time-slice reconstructions of ocean circulation changes on the continental shelf in the Nordic and Barents Seas during the last 16,000 cal yr B.P. Quaternary Science Reviews 27, 1476-1492.

Smith, A. J., Mienert, J., Bünz, S., Greinert J., 2014. Thermogenic methane injection via bubble transport into the upper Arctic Ocean from the hydrate-charged Vestnesa Ridge, Svalbard. Geochem. Geophys. Geosyst. 15, doi:10.1002/2013GC005179.

Stuiver, M., Reimer, P.J., 1993. Extended ^{14}C data base and revised CALIB 3.0 ^{14}C age calibration program. Radiocarbon 35, 215–230.

Stuiver, M., Reimer, P.J., Reimer, R., 2014. CALIB Radiocarbon CalibrationExecute, Version 7.0html, http://calib.qub.ac.uk/calib/.

Taylor, A.E., Dallimore, S.R., Hyndman, R.D., Wright, F., 2005. Comparing the
sensitivity of permafrost and marine gas hydrate to climate warming, in: Dallimore,
S.R., and Collett, T.S., (Eds.) Scientific results from the Mallik 2002 gas hydrate
production research well program, Mackenzie Delta, Northwest Territories,
Canada. Geological Survey of Canada Bulletin 585, 11 pp.

Thatcher, K.E., Westbrook, G.K., Sarkar, S., Minshull, T.A., 2013. Methane release
from warming-induced hydrate dissociation in the West Svalbard continental
margin. Journal of Geophysical Research B, Solid Earth 118 (1), 22-38.

Urey, H.C., Lowenstam, H.A., Epstein, S., McKinney, C.R., 1951. Measurement of
paleotemperatures and temperatures of the Upper Cretaceous of England, Denmark
and southeastern United States. Geological Society of America Bulletin 62, 399–
416.

Walker, M.J.C., Björck, S., Lowe, J.J., Cwynar, L.C., Johnsen, S.J., Knudsen, K.L.,
Wohlfarth, B., INTIMATE Group, 1999. Isotopic 'events' in the GRIP ice core: a
stratotype for the Late Pleistocene. Quaternary Science Reviews, 18, 1143–1150.

Werner, K., Spielhagen, R.F., Bauch, D., Hass, H.C., Kandiano, E., Zamelczyk, K., 2011.
Atlantic Water advection to the eastern Fram Strait — Multiproxy evidence for late
Holocene variability. Palaeogeography, Palaeoclimatology, Palaeoecology, 308,
264–276.

Westbrook G.K., Thatcher, K.E., Rohling, E.J., Piotrowski, A.M., Palike, H.,
Osborne,A.H., Nisbet, E.G., Minshull, T.A., Lanoiselle, M., James, R.H.,
Huhnerbach, V., Green, D., Fisher, R.E., Crocker, A.J., Chabert, A., Bolton, C.,
Beszczynska-Moller, A., Berndt, C., Aquilina, A., 2009. Escape of methane gas

from the seabed along the West Spitsbergen continental margin. Geophysical Research Letters 36, L15608.

Westbrook, G.K., Chand, S., Rossi, G., Long, C, Bünz, S., Camerlenghi, A., Carcione, J.M., Dean, S., Foucher, J.P., Flueh, E., Gei, D., Haacke, R.R., Madrussani, J., Mienert, J., Minshull, T.A., Nouzé, H., Peacock, S., Reston, T., Vanneste, M., Zillmer, M. 2008. Estimation of gas-hydrate concentration from multi-component seismic data at sites on the continental margins of NW Svalbard and the Storegga region of Norway. Marine and Petroleum Geology 25, 744–758.

Wollenburg, J. E., Kuhnt, W., Mackensen, A., 2001. Changes in Arctic Ocean paleoproductivity and hydrography during the last 145 kyr: The benthic foraminiferal record. Paleoceanography 16, 65–77.

Wollenburg, J.E., Knies, J., Mackensen, A., 2004. High-resolution paleoproductivity fluctuations during the past 24 kyr as indicated by benthic foraminifera in the marginal Arctic Ocean. Palaeogeography, Palaeoclimatology, Palaeoecology 204, 209-238.

Wollenburg, J. E., Mackensen, A., Kuhnt, W., 2007. Benthic foraminiferal biodiversity response to a changing Arctic palaeoclimate in the last 24.000 years. Palaeogeography, Palaeoclimatology, Palaeoecology 255, 195–222.

Figure 1. - A. Location of core GC-26. B. The site of the bubble plume and core GC-26 (black dot) on the western side of one of several pockmarks aligned along the crest of the Vestnesa Ridge. Water depth derived from multibeam bathymetry. The line of the acoustic image of Figure 1C is shown by the fine dashed line. C. Acoustic (Simrad EK60) image of a bubble plume rising from the pockmark. High acoustic backscatter from the seabed and from the plume of bubbles is displayed in red-brown.

Figure 2. - Lithologic log and pore water geochemistry of core GC-26.

Figure 3. - Percentage distributions of the benthic foraminifera species that have been identified to provide crucial paleoceanographic information in sediment cores from the West Svalbard continental margin by Bauch et al. (2001), Wollenburg et al. (2004; 2007), Rasmussen et al. (2007) and Ślubowska-Woldengen et al., (2007; 2008) in which the relative abundance of foraminiferal species in core GC-26 has been tied to the limit of time intervals. See text for more details. Abbreviations: GS, Greenland (isotope) stadial; GI, GI: Greenland (isotope) Interstadial; YD, Younger Dryas; B-A, Bølling–Allerød.

Figure 4. - SEM micrographs showing: A. Foraminiferal calcitic test wall after cleaning with methanol (standard protocol for stable isotope measurements); note that both an outer thin calcitic cryptocrystalline overgrowth, which resembles the test, and the inner (primary wall) of the test are present (scale bar 50 μm). B. Close-up of the outer foraminiferal calcitic cryptocrystalline overgrowths shown in A (scale bar 10 μm). C. Fragment of the innermost part of the test after the application of the more extensive

cleaning protocol. Note that there is no longer evidence of any layers or tiny patina of carbonate cryptocrystalline overgrowths (scale bar 50μm).

Figure 5. - Stratigraphic scheme and stable isotope data for core GC-26. From left to right: (i) Benthic foraminiferal $\delta^{13}C$ and $\delta^{18}O$ composition of *Cassidulina neoteretis* and *Melonis barleeanum*; *C. neoteretis* samples were cleaned using both the standard (closed squares) and the more extensive (open squares) protocols (see text for details), together with the Methane Emission Events (MEEs); the age model obtained from ^{14}C dating is indicated by the black bold dashed line (ii) NGRIP $\delta^{18}O$ curve. iii) methane concentration from GISP2 ice core. iv) Stratigraphy obtained for GC-26. Dashed lines indicate chronological boundary.
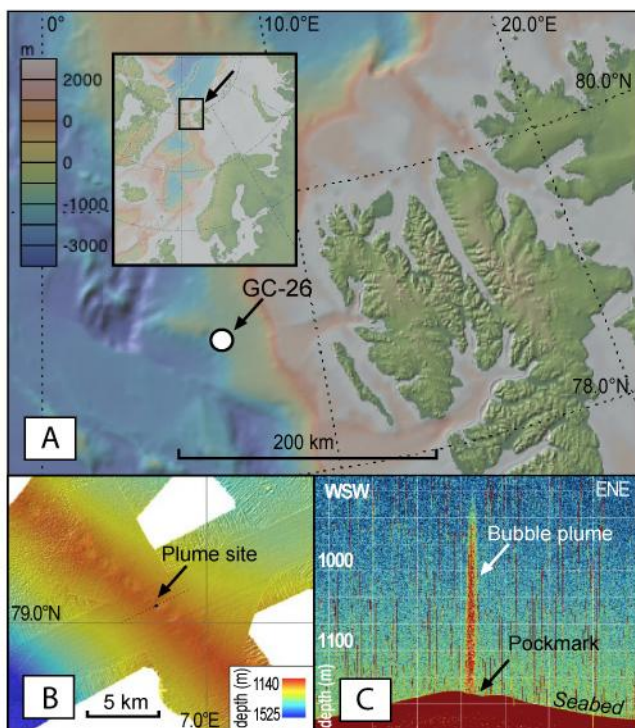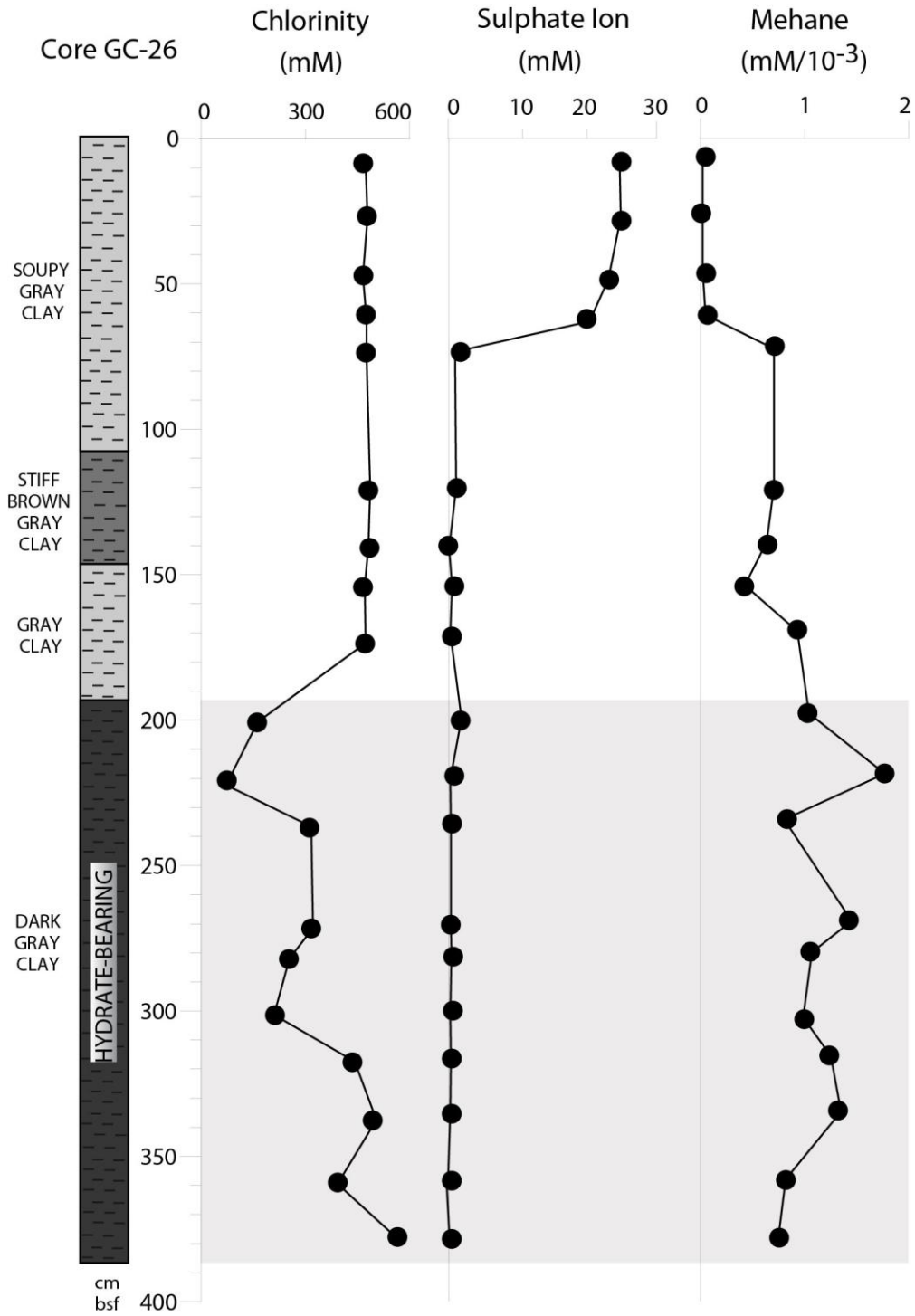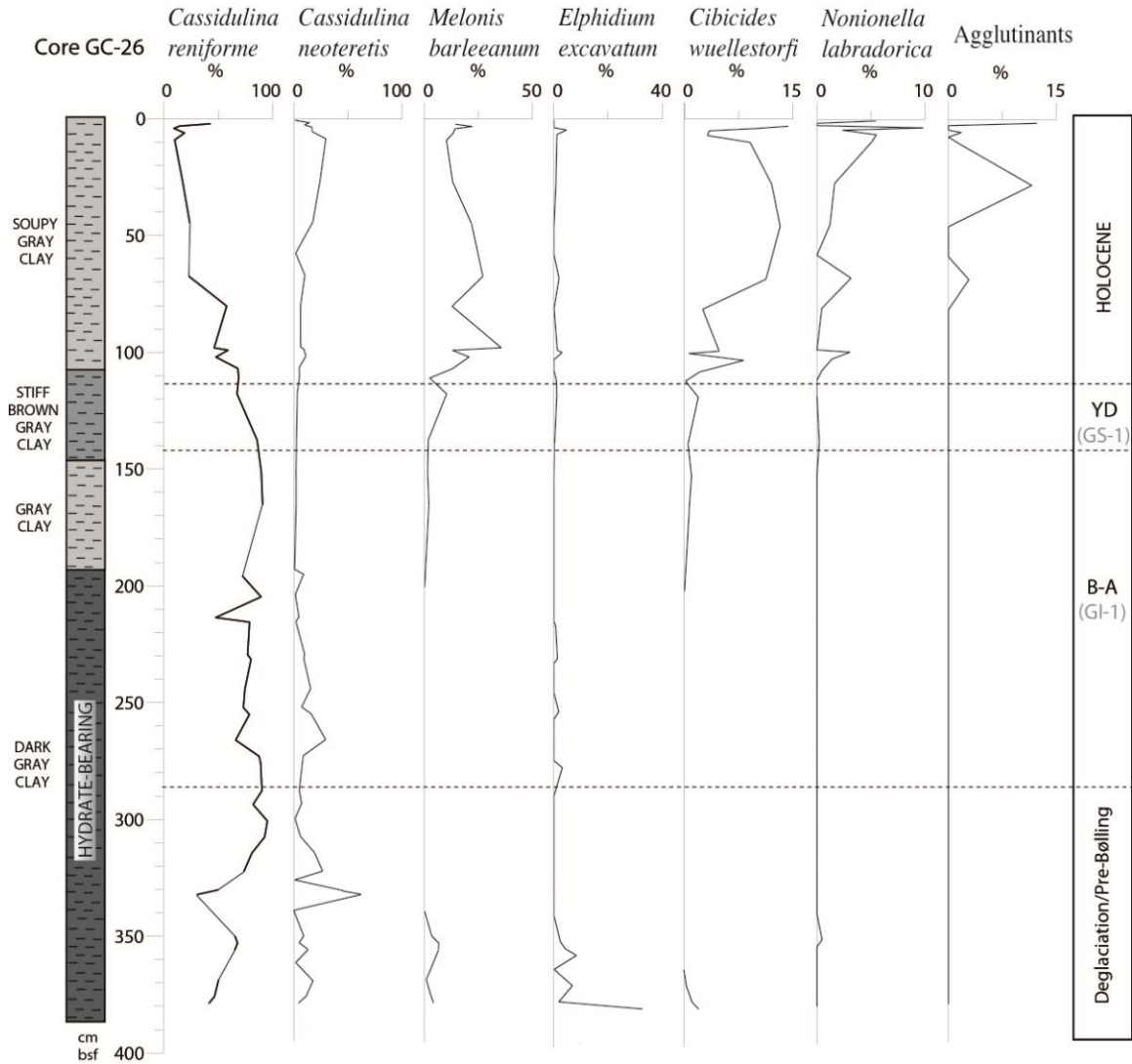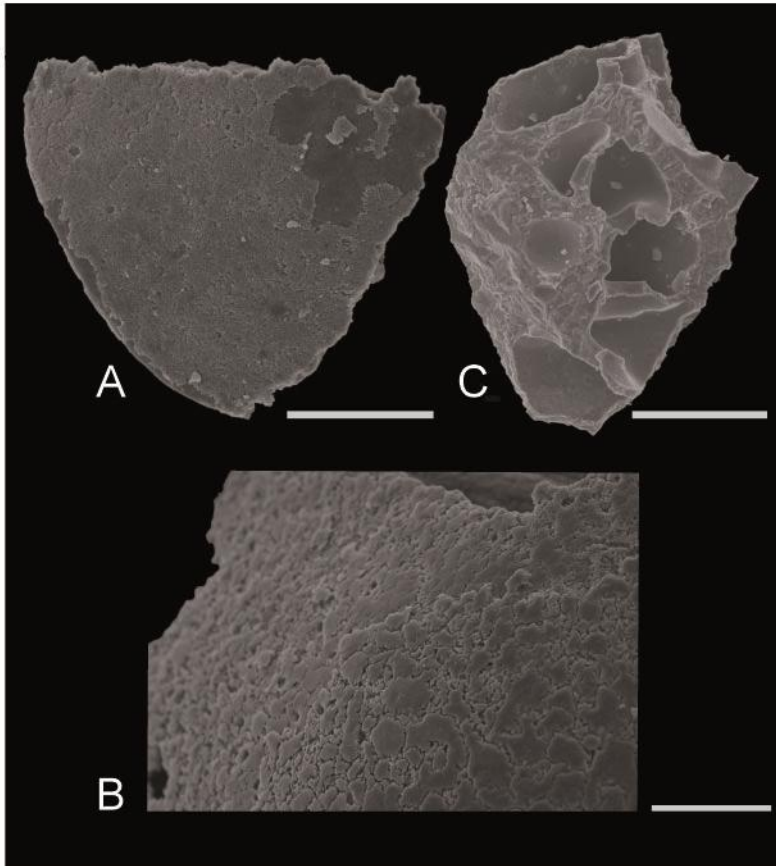
Figure 1

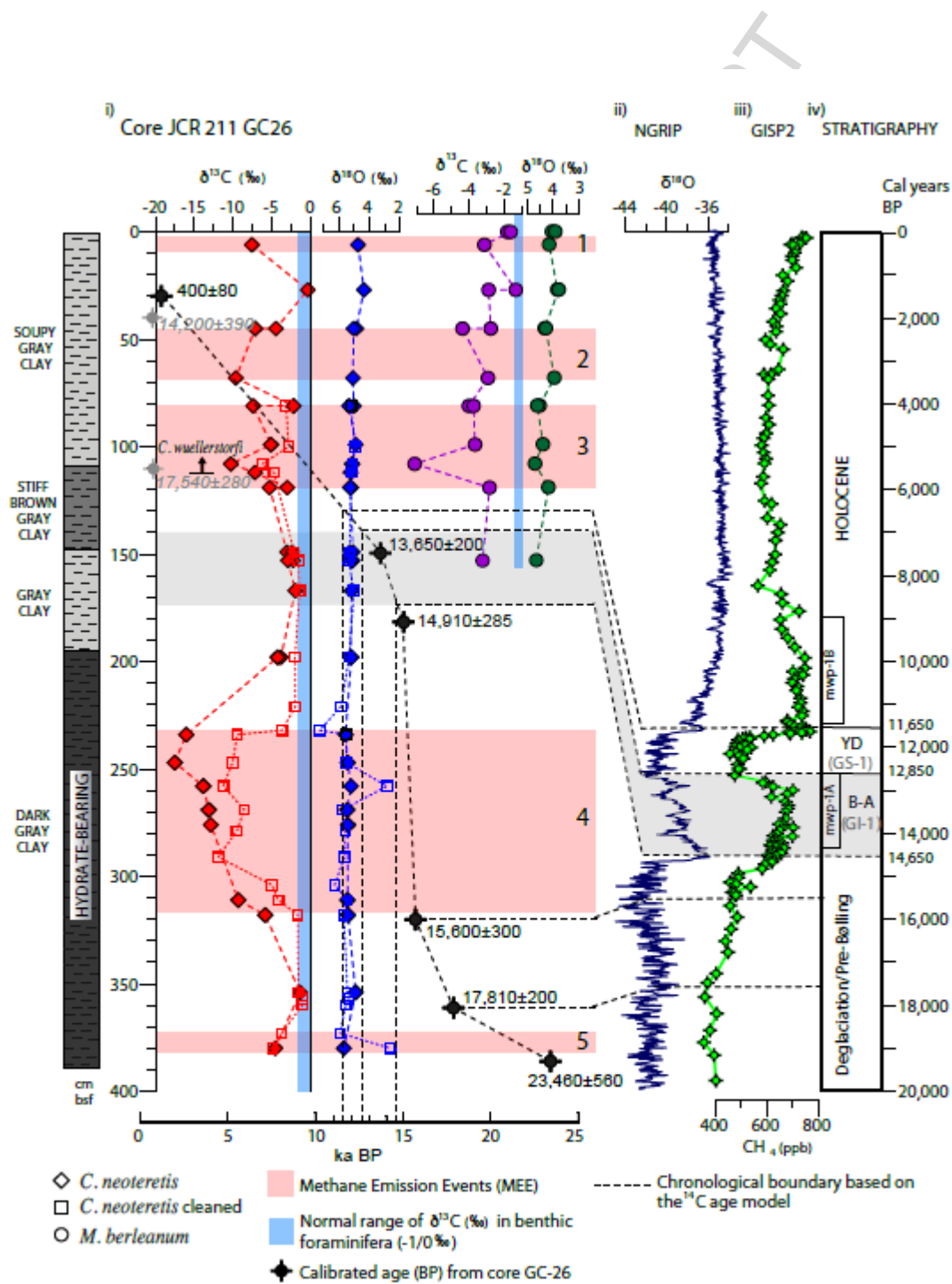Figure 2

Figure 3

Figure 4

Figure 5

Table 1. - Carbon and oxygen stable isotopic composition of benthic foraminifera recovered from core GC-26.

Depth in core (cm)	Cassidulina teretis#		Cassidulina teretis§		Melonis barleenum#	
	$\delta^{13}C$	$\delta^{18}O$	$\delta^{13}C$	$\delta^{18}O$	$\delta^{13}C$	$\delta^{18}O$
0					-1,82	4,01
0					-1,63	3,88
6	-7,52	4,61	N.D.*	N.D.*	-3,12	4,12
27	-0,28	4,23	N.D.*	N.D.*	-1,34	3,80
27					-2,88	3,75
45	-4,41	4,72	N.D.*	N.D.*	-2,76	4,29
45	-7,11	4,9	N.D.*	N.D.*	-4,36	4,25
68	-9,60	4,94	N.D.*	N.D.*	-2,92	3,92
81	-2,13	4,89	N.D.*	N.D.*	-4,00	4,49
81	-7,35	5,19	-3.11	5.06	-3,73	4,58
99	-5,05	4,77	N.D.*	N.D.*	-3,65	4,36
100	N.D.*	N.D.*	-2.76	4.81		
108	-10,25	4,99	-6.17	4.98	-7,07	4,67
112	-7,12	5,09	-4.66	5.02		
119	-2,95	5,06	N.D.*	N.D.*	-2,83	4,15
119	-5,24	5,12	N.D.*	N.D.*		
149	-2,98	4,94	-2.05	5.17		
149	-2,32	5,14	N.D.*	N.D.*		
153	-2,19	4,95	-1.53	5.23	-3,22	4,62
153	-2,87	5,05	N.D.*	N.D.*		
167	-1,90	5,03	-1.33	4.88		
198	-3,78	5,09	-1.94	5.19		
198	-4,18	5,05	N.D.*	N.D.*		
221	N.D.*	N.D.*	-1.9	5.72		
232	N.D.*	N.D.*	-3.64	7.1		
234	-16,03	5,42	-9.42	5.38		
247	-17,52	5,28	-10.03	5.36		
258	-13,82	5,07	-11.25	2.74		
269	-13,12	5,31	-8.51	5.6		
276	-12,85	5,26	N.D.*	N.D.*		
279	N.D.*	N.D.*	-9.5	5.42		
291	N.D.*	N.D.*	-11.88	5.49		
304	N.D.*	N.D.*	-4.92	6.13		
311	-9,28	5,30	-4.12	5.3		
318	-5,80	5,26	-1.59	5.53		
354	-1,27	4,77	-1.5	5.3		
357	N.D.*	N.D.*	-1.03	5.2		
360	N.D.*	N.D.*	-0.99	5.41		
373	N.D.*	N.D.*	-3.67	5.77		

380	-4,49	5,53	-4.83	2.52

\# tests cleaned with methanol

§ tests subject to more extensive cleaning (see text for details)

*N.D.= not determined

Table 2. - Radiocarbon data for core GC-26.

Depth in core (cm)	AMS Laboratory Code	Carbonate	Uncorrected AMS^{14}C Age From Direct Dating	ΔR	Corrected age (2-sigma) ^{14}C ky BP	Mean corrected age (2-sigma) ^{14}C ky BP	δ^{13}C (‰ VPDB)
29	OS-110568	Planktonic foraminifera	775±25	7±11	320-17467	400±80	N.D.[#]
38	OS-110566	Planktonic and benthic foraminifera	12700±100	105±24	13810-14581	14200±390	N.D.[#]
108	OS-95389	Planktonic and benthic foraminifera	14900±80	105±24	17261-17821	17540±280	-10.98
153	OS-95390	Planktonic and benthic foraminifera	12300±75	105±24	13447-13845	13650 ± 200	-2.28
181	OS-110385	Planktonic and benthic foraminifera	13100±50	105±24	14626-15196	14910± 285	N.D.[#]
203		Planktonic and benthic foraminifera	N.D.[#]	105±24	N.D.[#]	N.D.[#]	N.D.[#]
321	OS-95387	Planktonic and benthic foraminifera	13550±80	105±24	15299-15898	15600±300	-4.11
361	OS-110386	Planktonic and benthic foraminifera	15150±65	105±24	17615-18013	17810±200	N.D.[#]
386	OS-110561	Planktonic foraminifera	19900±230	7±11	22903-24024	23460±560	N.D.[#]

N.D.[#] = not determined.

Highlights

Negative $\delta^{13}C$ in benthic foraminifera indicate methane emissions in the Arctic.

Methane emissions have occurred over the past 23,500 years BP in the Vestnesa Ridge.

The methane emission events show an apparent correlation with climatic events.

One or more geological processes control the supply of methane to the seabed.